

# **Controllable Fabrication of Magnetic Core-Shell Nanocomposites with High Peroxide Mimetic Properties for Bacterial Detection and Antibacterial Applications**

Qiusen Han<sup>[-],a,b</sup>, Xinhuan Wang<sup>[-],a</sup>, Xueliang Liu<sup>a</sup>, Wei Xiao<sup>a</sup>, Shuangfei Cai<sup>a</sup>, Chen Wang<sup>\*a,b</sup>,  
Rong Yang<sup>\*a,b</sup>

- a. CAS Key Lab for Biomedical Effects of Nanomaterials and Nanosafety, Center of Materials Science and Optoelectronics Engineering, CAS Center for Excellence in Nanoscience, National Center for Nanoscience and Technology, University of Chinese Academy of Sciences, Beijing, 100049, P. R. China
- b. Sino-Danish College, Sino-Danish Center for Education and Research, University of Chinese Academy of Sciences, Beijing, 100049, P. R. China

\* Corresponding author: yangr@nanoctr.cn, wangch@nanoctr.cn

† Supporting information for this article is available

[-] These authors contributed equally to this work.

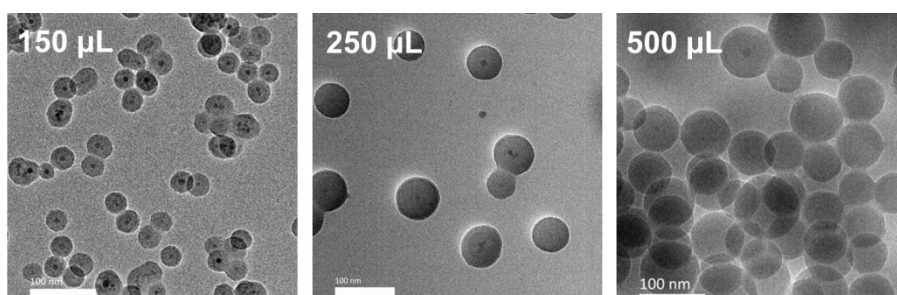


Fig.S1 The influence of TEOS amount on SiO<sub>2</sub> layer thickness.

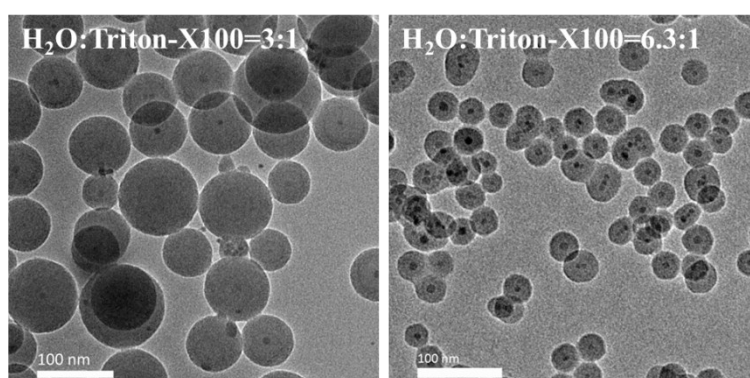


Fig.S2 The influences of the ratios of H<sub>2</sub>O and Triton-X100 on SiO<sub>2</sub> layer thickness.

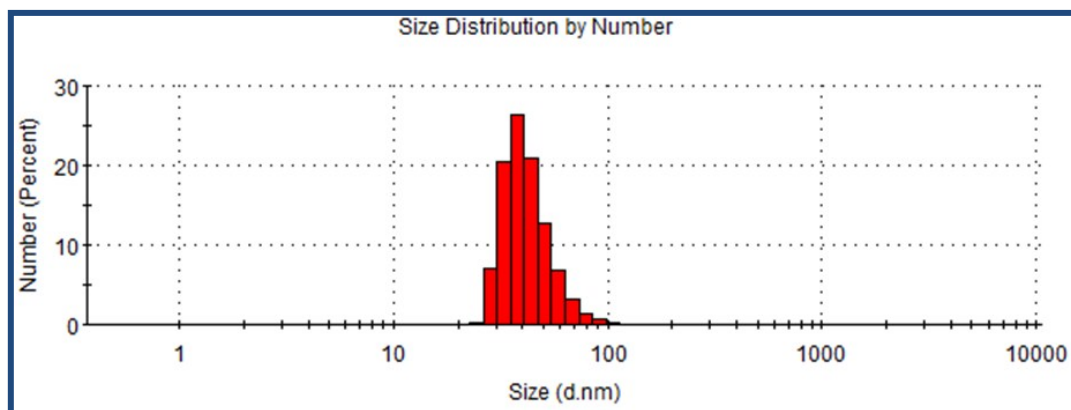


Fig.S3 DLS of  $\text{Fe}_3\text{O}_4@\text{SiO}_2\text{-Pt}$  nanocomposites.

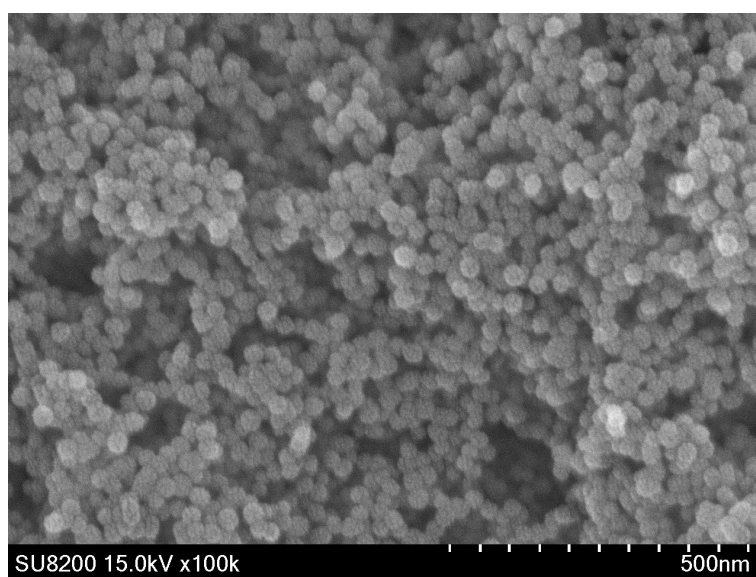


Fig.S4 SEM image of  $\text{Fe}_3\text{O}_4@\text{SiO}_2\text{-Pt}$  nanocomposites.

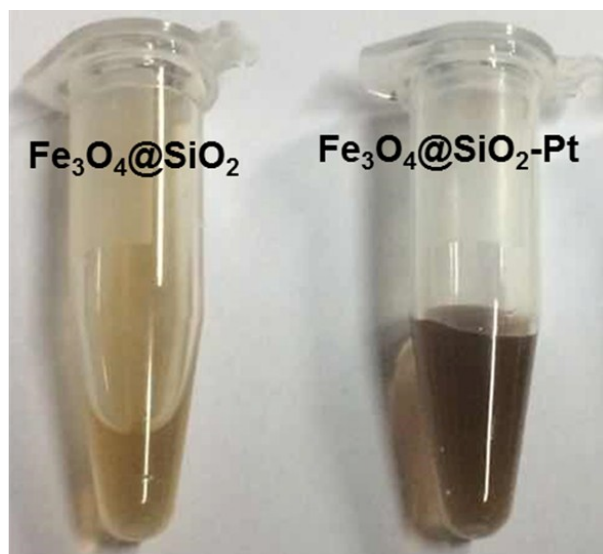


Fig.S5 Photo images of  $\text{Fe}_3\text{O}_4@\text{SiO}_2$  and  $\text{Fe}_3\text{O}_4@\text{SiO}_2\text{-Pt}$  nanocomposites.

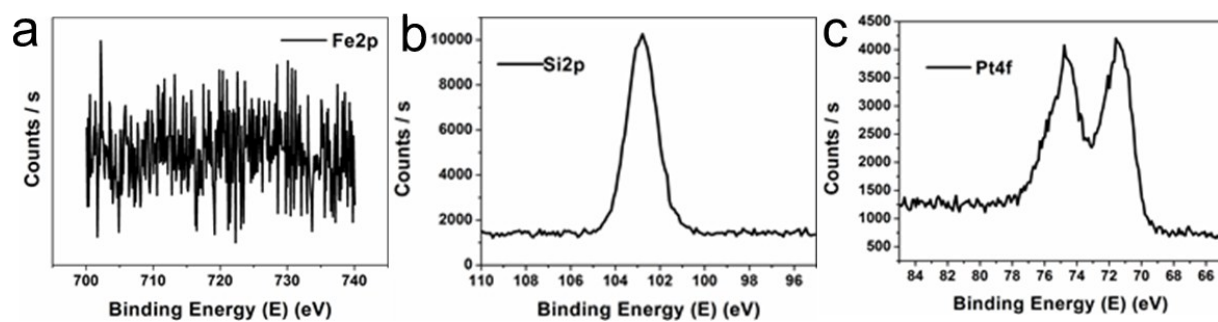


Fig.S6 XPS of  $\text{Fe}_3\text{O}_4@\text{SiO}_2\text{-Pt}$  nanocomposites.

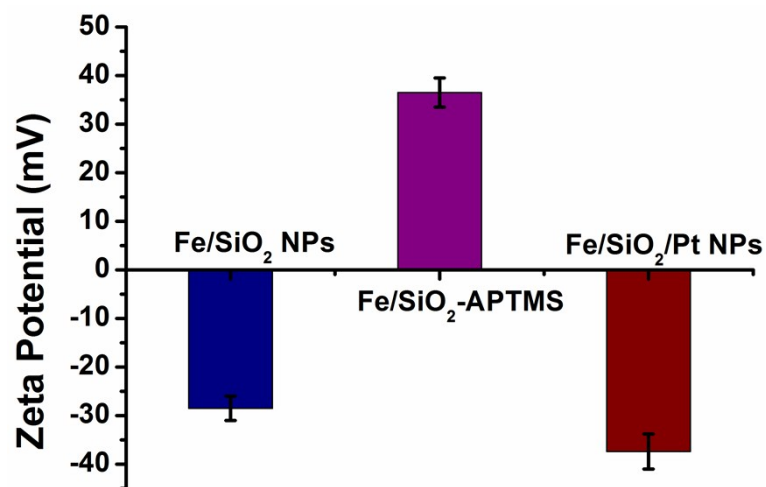


Fig.S7 Zeta potential analysis of Fe<sub>3</sub>O<sub>4</sub> with various modification.

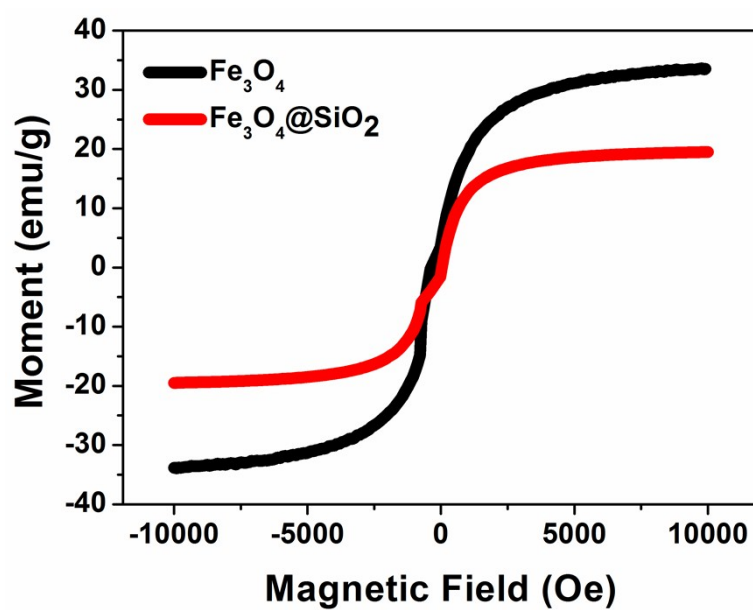


Fig.S8 The M (H) hysteresis curve for Fe<sub>3</sub>O<sub>4</sub> and Fe<sub>3</sub>O<sub>4</sub>@SiO<sub>2</sub> NPs.

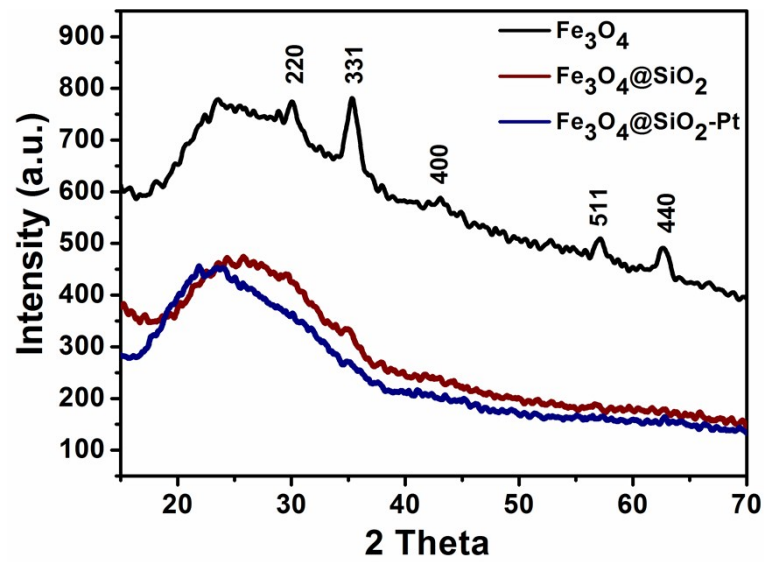


Fig.S9 XRD of Fe<sub>3</sub>O<sub>4</sub>@SiO<sub>2</sub>-Pt nanocomposites.

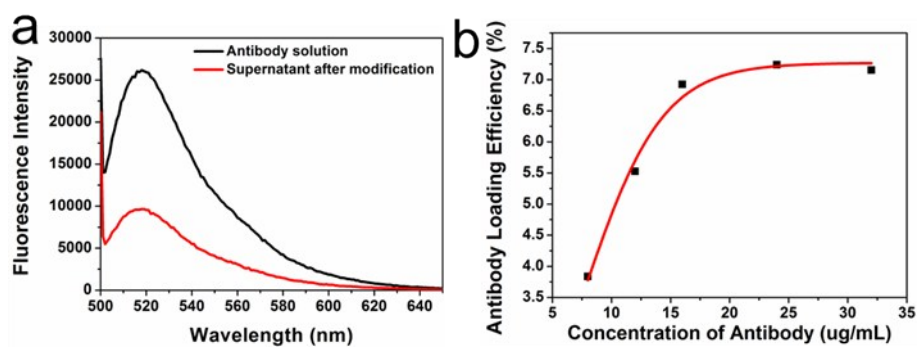


Fig.S10 Anti-*S.aureus* antibody modification of Fe<sub>3</sub>O<sub>4</sub>@SiO<sub>2</sub>-Pt nanocomposites.

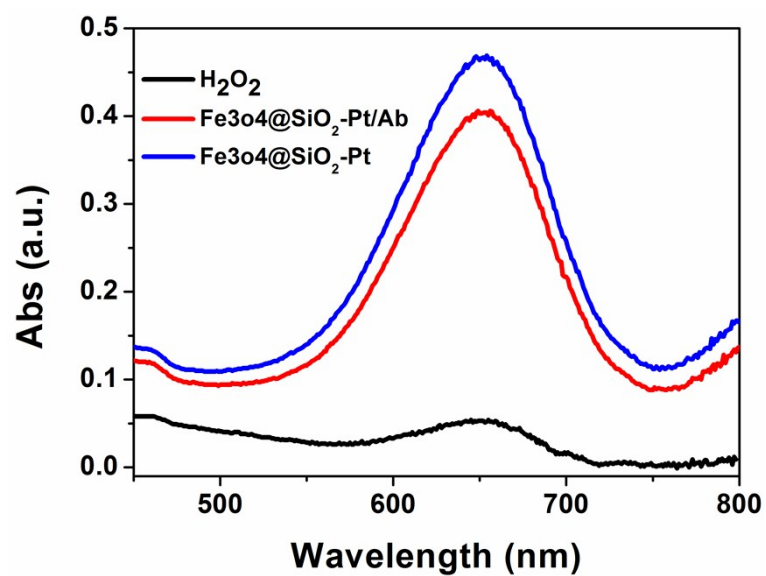


Fig.S11 UV-Vis absorption spectra of oxidize TMB treated with various samples.

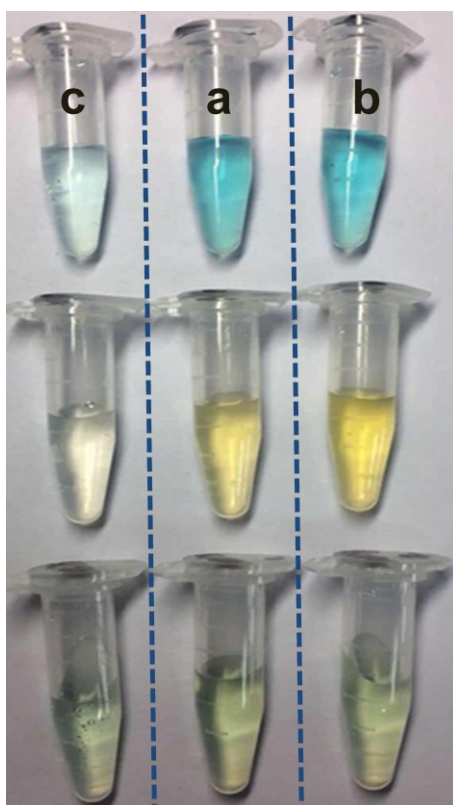


Fig.S12 Photo images of color changes treated with  $\text{Fe}_3\text{O}_4@\text{SiO}_2\text{-Pt}$  (a) and  $\text{Fe}_3\text{O}_4@\text{SiO}_2\text{-Pt/Ab}$  (b), (c) negative control.

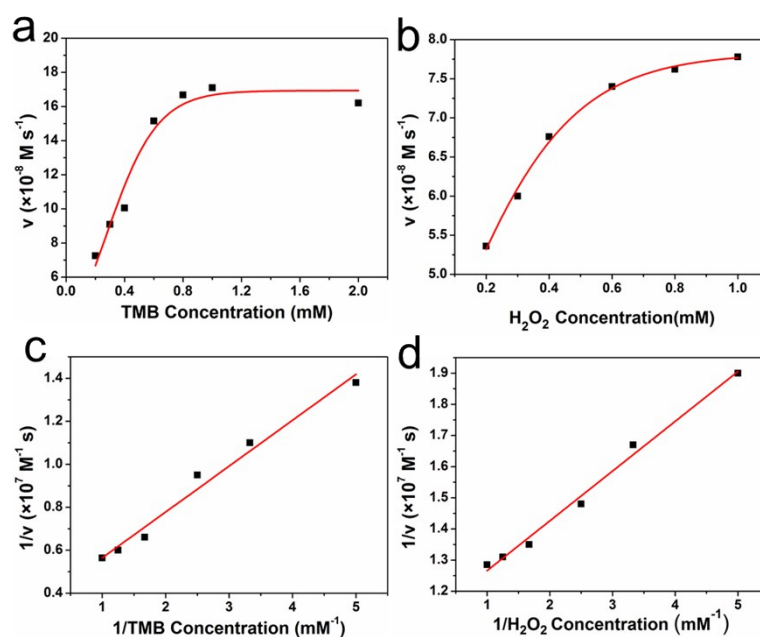


Fig.S13 Steady-state kinetic analysis using Michaelis-Menten model (a, b) and Lineweaver-Burk model (c, d) for  $\text{Fe}_3\text{O}_4@\text{SiO}_2\text{-Pt}$  nanocomposites.

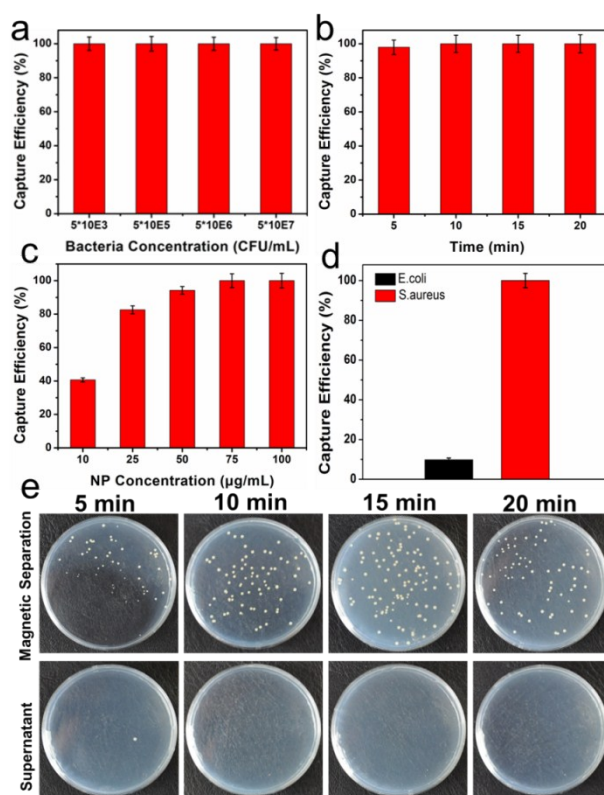


Fig.S14 Bacteria separation ability of  $\text{Fe}_3\text{O}_4@\text{SiO}_2\text{-Pt}$  nanocomposites.